Physicochem. Probl. Miner. Process. 49(2), 2013, 397−405

www.minproc.pwr.wroc.pl/journal/

Physicochemical Problems of Mineral Processing

ISSN 1643-1049 (print)
ISSN 2084-4735 (online)

Received April 28, 2012; reviewed; accepted August 30, 2012

ANALYSIS OF LARGE PARTICLE SIZES USING A MACHINE VISION SYSTEM

Zelin ZHANG, Jianguo YANG, Xiaolan SU, Lihua DING

School of Chemical Engineering and Technology, China University of Mining and Technology, Xuzhou 221116, Jiangsu, China; zhangzelin3180@163.com; scetyjg@126.com.

Abstract: Many methods based on machine vision were used to estimate coarse particles size distribution in recent years, but comparison of accuracy parameters representing particle size has not been carried out and a related representing analysis has not been yet proposed. Nine parameters were investigated. The results indicated the minor axis of equivalent ellipse and breadth of the best-fit rectangle were the most suitable for representing particle size. The former accuracy ratio was 86.43% and the latter accuracy ratio was 85.39%, while the accuracy of other parameters was less than 70%. A related representing analysis was proposed to explain this phenomenon. This research is instructive and meaningful for the size distribution estimation by machine vision.

Keywords*: machine vision, particle size distribution, equivalent ellipse, best-fit rectangle, representing analysis*

Introduction

Particle size and size distribution are important variables in many industrial sectors (Tasdemir et al., 2011; Zhang et al., 2012), especially in mining and mineral processes. Most mineral processing operations rely on the size distributions measurement as a key factor in improving process efficiencies (Xia et al., 2012a; Xia et al., 2012b). Sieving has been used to measure particle size distribution traditionally, but it is very time-consuming and cannot be quick enough to provide real-time feedback information to direct production. So machine vision has been used for particle size measurement in the last twenty years.

Many problems such as the way of image acquisition, the algorithm of image segmentation, parameters of particle size and error correction of the system had all been extensively investigated in recent years. However, a comparison of all parameters in accuracy aspect has not been carried out and related representing analysis has not yet proposed. Authors argue that the size parameters extracted from images to represent

http://dx.doi.org/10.5277/ppmp130202

sieving particle size should satisfy two demands, i.e., be rotationally-invariant and have a selecting basis.

In image analysis, different ways of measuring particle size, such as equivalent circle diameter (Maerz et al., 1987; Mcdermott et al., 1989; Grannes et al., 1986; Donald and Kettunen, 1996; Maerz et al., 1996; Rholl et al., 1993), maximum size (Montoro et al., 1993; Ord et al., 1989; Kemeny et al., 1994), size of equivalent ellipse (Girdner et al., 1996; Schleifer et al., 1993), Ferret diameter (Kwan et al., 1999; Mora et al., 1998; Mora et al., 2000; Al-Thyabat et al., 2006; Al-Thyabat et al., 2007) and best-fit rectangle (Wang, 2006; Tobias et al., 2012) have been used. All the above parameters are rotationally-invariant, but are optionally selected to estimate size distribution with no representing analysis and selecting basis.

In this paper, 467 coal particles in four size fractions were selected through a strict screening to compare the accuracy of the above mentioned parameters, and a representing analysis combined with a screening principle was proposed to explain the results.

Experiments

Sample preparation

The experiment sample was anthracitic coal from the Tai-Xi coal preparation plant in China. Basically, the sieving operation attempts to divide the coal sample into fractions, each consisting of particles within specific size limits. In China's coal cleaning standards, the mesh apertures are 100, 50, 25, 13, 6, 3, 0.5 mm. When necessary, the mesh apertures can increase or decrease, so a series of sieves with square apertures 3, 6, 13, 25, 50 mm were used in our experiment. As to the coal particles smaller than 3 mm, the outline accuracy by digital image processing is low, and the particles greater than 50 mm are not suitable for experiment and test. For the reasons given above, the particles smaller than 3 mm and greater than 50 mm were discarded. 120 particles (3–6 mm), 146 particles (6–13 mm), 109 particles (13–25 mm) and 92 particles (25–50 mm) were selected to accomplish this research.

Image acquisition and parameters calculation

A high quality picture of the coal particles is needed before any digital image processing is performed. Some researchers noted the shadows cast by the objects, and the interior texture could be confusing to edge detection algorithms (Wang, 2006; Guyot et al., 2004; Casali et al., 2001). A backlit system, shown in Fig. 1A, was built to eliminate these problems. This system was designed as a closed box for avoiding the outside light effect. Digital camera (Nikon S220) was put in the camera hole of this system, and we fixed the height from the hole to the platform as 41.5 cm, just right above of the sample platform. Four fluorescent lamps (TCL 8W) were set equidistantly under the sample platform. Figure 1B is an image of one coal particle taken in the normal daylight, and Fig. 1C is an image of the same coal particle taken in the

backlit system. It is obvious that the image taken in the backlit system can eliminate the shadow and the interior texture, which provide a good basis for extracting features accurately.

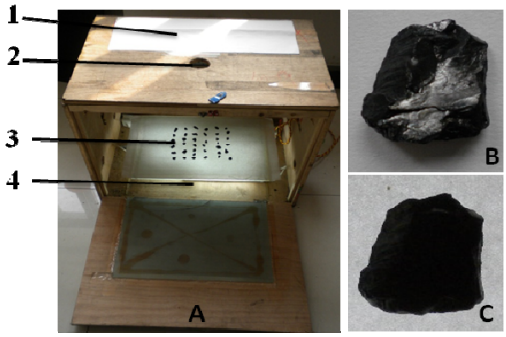

Fig. 1. A – backlit system, B – image of one coal particle taken in normal daylight, C – image of the same coal particle taken in backlit system; 1 – closed box, 2 – camera hole, 3 – sample platform, 4 – lights

The pixel size of the captured image is 1024×768. The image from Fig. 2 (A) was used to measure the shooting coverage and the conversion ratio between pixel size and actual size. The shooting coverage is 366 mm×274.5 mm, and one pixel is approximately equal to 0.357 mm. When the coal particles are placed on the sample platform, they are carefully spread out, making certain that they are in the stable position and without touching or overlapping each other to insure the accurate edge extraction. Figure 2 (B) is a gray histogram of the image after removing the ruler seen in Fig. 2 (A). The optimal threshold was determined manually as 50 for the twin-peaks method. Sometimes there will be several dirty spots or dust on the platform. In this case the area threshold will be used to remove these isolated micro-regions and filling processes will be used to fill the interior of particles completely. Through the above image processes, all our images can be segmented accurately, like in Fig. 2(C). In this part, some researchers used some methods to segment images, like filtering, dilating, eroding, top-hat, bottom-hat and watershed and so on (Al-Thyabat et al., 2007; Banta et al., 2003). Many morphological processes will cause an inaccurate outline of particles because the regions handled by structure elements chosen in these operations may be changed, especially during dilating and eroding processes. So, we used in our experiments no touching particles and the simple but credible segmentation method to insure the experiment precision.

Nine parameters were investigated. A sketch map of parameters which are easy to express were shown in Fig. 2(D):

D_A – equivalent circle diameter: the circle area is equal to the target area,

$D_{\max}$ – maximum size: the maximum distance between two pixels on the perimeter,

D_{major} – major axis of equivalent ellipse: the length of the major axis of the ellipse that has the same normalized second central moments as the target region,

D_{minor} – minor axis of equivalent ellipse: the length of the minor axis of the ellipse that has the same normalized second central moments as the target region,

D_{mean1} – the average of d_{major} and d_{minor},

D_F – Ferret's diameter: the mean value of distances cross the centroid between two parallel tangents which are on opposite sides of the target region in 0°, 45°, 90° and 135°,

D_B – the breadth of best-fit rectangle of target region. The method of best-fit rectangle is a combination of the Ferret method and the least 2nd moments minimization, requiring only calculation of the three moments about the center of gravity, and maximum and minimum co-ordinates in a co-ordinate system oriented in the direction of the axis of the least 2nd moments, and a simple area ratio (Weixing, 2006),

D_L – the length of best-fit rectangle of target region,

D_{mean2} – the average of dB and dL.

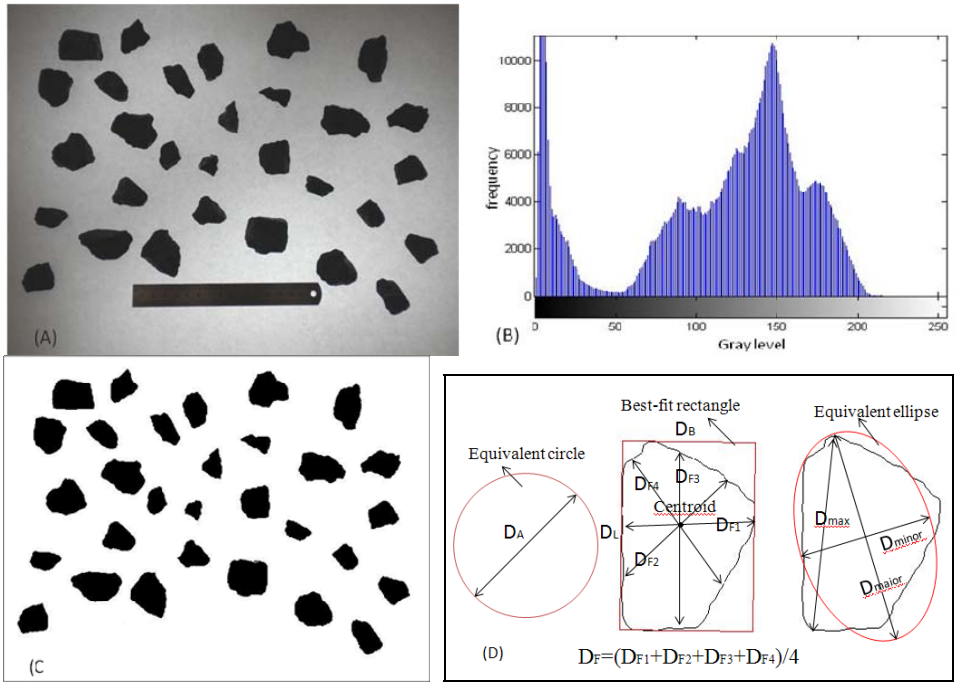

Fig. 2. Image acquisition and processing: (A) coal particles image taken in the backlit system, (B) gray histogram of image after removing ruler in the image (A), (C) binary of image (B) processed by twin-peaks method and removing isolated points, (D) sketch map of D_A, D_F, D_B, D_L, D_{max}, D_{major} and D_{minor}

In order to test and verify the accuracy of this image technique, the length and breadth of best-fit rectangle were used to carry out the comparison. A vernier caliper, minimum range of which is 0.02 mm, was used to measure the actual length and breadth of best-fit rectangle according to the rectangular position after image proc-

esses, like Fig. 3A. Figures 3B and 3C show the actual measurement of breadth and length of one coal particle. Twelve coal particles, three in each size fraction, were chosen randomly to test and verify the accuracy using the above method, and the results were shown in Table 1. The average and variance of absolute value of errors were 0.23 mm and 0.03 mm^2, respectively, indicating that the difference between actual size and estimated size is small. Furthermore, the T-test was used to verify whether the average error is zero. The significance level α is determined as 0.05. The T-value and p-value are 0.4934 and 0.6264, respectively, indicating that the average error can be considered as zero in the above significance level, that is, the errors' fluctuation is normal. All the results show that the accuracy of this image analysis is high and satisfied.

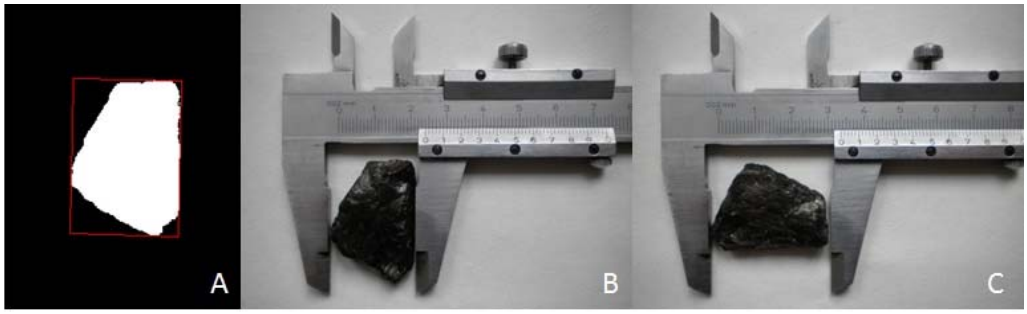

Fig. 3. A. The best-fit rectangle of one coal particle, B. Measuring the actual breadth of this particle best-fit rectangle, C. Measuring actual length of this particle best-fit rectangle, according to the rectangular position of image A

Table 1. Accuracy test of breadth and length of best-fit rectangle by image technique according to actual measurement by vernier caliper

Num	Length of best-fit rectangle, mm			Breadth of best-fit rectangle, mm		
	Actual	Estimation	Error	Actual	Estimation	Error
1	5.10	5.12	–0.02	3.30	3.59	–0.29
2	5.26	5.06	0.2	3.16	3.36	–0.2
3	4.56	4.32	0.24	4.08	3.95	0.13
4	6.58	6.21	0.37	6.00	5.81	0.19
5	10.36	9.95	0.41	8.04	7.88	0.16
6	7.96	7.86	0.1	6.20	5.91	0.29
7	14.02	14.09	–0.07	6.70	6.81	–0.11
8	21.10	21.08	0.02	20.20	20.43	–0.23
9	20.66	20.49	0.17	18.80	18.67	0.13
10	28.54	28.53	0.01	24.40	23.78	0.62
11	33.24	33.17	0.07	23.10	23.54	–0.44
12	44.06	44.51	–0.45	33.30	33.89	–0.59
Average of absolute value of errors, mm		0.23		Variance of absolute value of errors, mm^2		0.03
t-value		0.4934		p-value		0.6264

Results and discussion

Totally 467 coal particles in four size fractions were selected through strictly screening to compare the accuracy of the investigated nine parameters. The accuracy ratio of each parameter in each size fraction was calculated as follows:

$$\text{Accuracy ratio} = \frac{\text{Correct number}}{\text{Total number}} \times 100\% . \tag{1}$$

The results shown in Fig. 4 indicate that D_{minor} and D_{B} were more suitable to represent the real particle size. The mean value of D_{B} accuracy ratio is 86.43%, and the mean value of D_{minor} accuracy ratio is 85.39%. The others were no more than 70%.

Particle is a 3-D object having length, width and thickness. D_{minor} and D_{B} were like the width of particles. Width must be smaller than the length. Weixing (2006) indicated that the particle width distribution curve is between the length and thickness curves. Authors verified this phenomenon previously. The real thicknesses of 496 particles were calculated by their real mass, real density and projected area. The width is instead of the breadth of the best-fit rectangle because it is near the real width. Figure 5 shows the results of comparing the real thickness and the breadth of the best-fit rectangle, indicating most particles' thickness are smaller than the width.

In the process of on-line analysis, particles are constantly shaking on the belt, so most particles stand on the stable side, i.e. sit on the biggest bottom area of particle. Of course the collision between particles will also affect the particle standing way. In the laboratory, particles lie mostly on the biggest bottom area, so length and width of the projected area are almost bigger than particle thickness. Thus:

$$\text{Thickness} \le \text{Width} \le \text{Length}.$$

When particles pass through a screen hole, according to the screening principle, there are two sizes smaller than the size of the screen hole. Therefore, the width of the particle determines whether this particle can pass through the screen hole. The values of D_{minor} and D_{B} are near the width of particles, so they are accurate for the analysis.

Conclusion

A set of 496 particles was selected from four size fractions by accurate sieving to compare the accuracy of representing the particle size by nine parameters. Results indicated the D_{minor} and D_{B} were the most suitable to represent the real particle size. The mean value of D_{B} accuracy ratio was 86.43%, and the mean value of D_{minor} accuracy ratio was 85.39%. The mean values of others parameters were no greater than 70%. The representing analysis combined with screening principle was proposed to

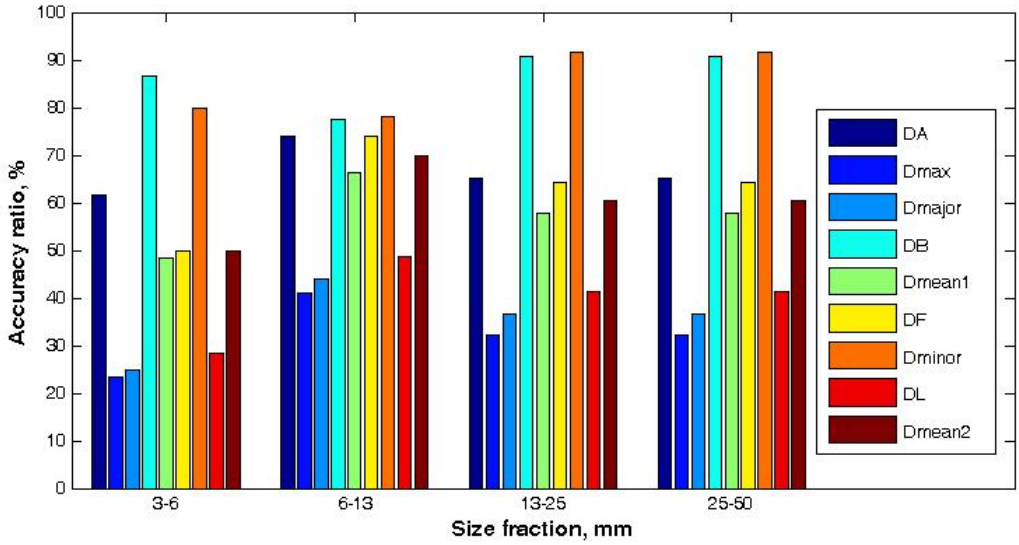

Fig. 4. A comparison of the accuracy of nine parameters in each size fraction

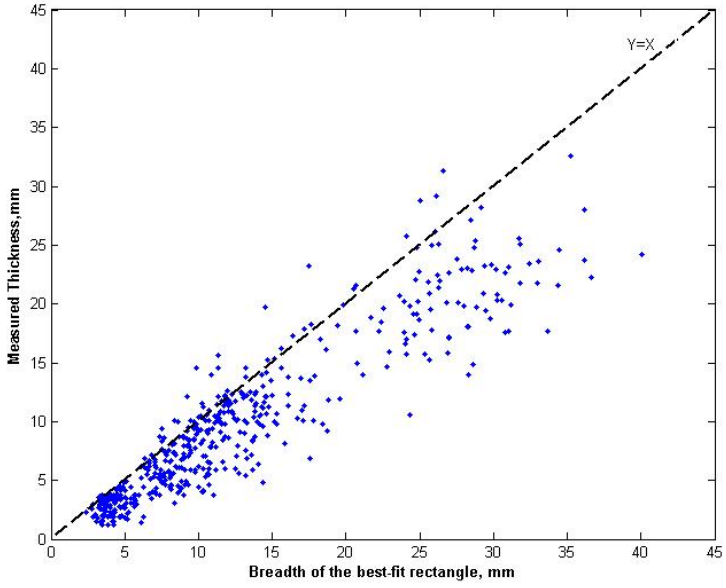

Fig. 5. Real thickness vs. breadth of the best-fit rectangle for the 496-particle sample

explain the results. This research is instructive and meaningful for the size distribution estimation by a machine vision system, especially for the coarse coal particles, based on which the on-line analysis for size distribution can be improved.

Acknowledgments

The authors would like to thank the Creative Research Groups Science Fund of the National Natural Science Foundation of China (No. 50921002)

References

AL-THYABAT S., MILES N.J., 2006. *An improved estimation of size distribution from particle profile measurements*. Powder Technology, 166, 152–160.

AL-THYABAT S., MILES N.J., KOH T.S., 2007. *Estimation of the size distribution of particles moving on a conveyor belt*. Minerals Engineering, 20, 72–83.

BANTA L., CHENG K., ZANIEWSKI J., 2003. *Estimation of limestone particle mass from 2D images*, Powder Technology, 132, 184–189.

CASALI A., GONZALEZ G., VALLEBUON G., PEREZ C., VARGAS R., 2001. *Grindability Softsensors based on Lithological Composition and On-Line Measurements*. Minerals Engineering, 14, 689-700.

DONALD C., KETTUNEN B.E., 1996. *On-line size analysis for the measurement of blast fragmentation*. In: J.A. Franklin, T. Katsabanis (Eds.), *Measurement of Blast Fragmentation*, Rotterdam, Balkema, 175–177.

GIRDNER K.K., KEMENY J.M., SRIKANT A., MCGILL R., 1996. *The split system for analyzing the size distribution of fragmented rock*. In: J.A. Franklin, T. Katsabanis (Eds.), *Measurement of Blast Fragmentation*, Rotterdam, Balkema, 101–108.

GRANNES S.G., 1986. *Determine size distribution of moving pellets by computer image processing*. In: R.V. Ramani (Ed.), *Proceedings of the 19th Application of Computers and Operations Research in Mineral Industry*, Soc. Mining Engineers, Inc., 545–551.

GUYOT O., MONREDON T., LAROSA D., BROUSSAUD A., 2004. *VisioRock, an Integrated Vision Technology for Advanced Control of Comminution Circuits*. Minerals Engineering, 17, 1227-1235.

KEMENY J., 1994. *A practical technique for determining the size distribution of blasted benches, waste dumps, and heap-leach sites*. Mining Engineering, 46, 1281–1284.

KWAN A.K.H., MORA C.F., CHAN H.C., 1999. *Particle shape analysis of coarse aggregate using digital image processing*. Cement and Concrete Research, 29 (9), 1403–1410.

MAERZ N.H., FRANKLIN J.A., ROTHENBURG L., COURSEN D.L., 1987. *Measurement of Rock Fragmentation by Digital Photoanalysis*. 5th. Int. Cong. Int. Soc. Rock Mech., 1, 687–692.

MAERZ N.H., PALANGIO T.C., FRANKLIN J.A., 1996. *WipFrag image based granulometry system*. In: J.A. Franklin, T. Katsabanis (Eds.), *Measurement of Blast Fragmentation*, Rotterdam, Balkema, 91–99.

MCDERMOTT C., HUNTER G.C., MILES N.J., 1989. *The application of image analysis to the measurement of blast fragmentation*. Proceedings of the Surface Mining – Future Concepts, Nottingham University, Marylebone Press, Manchester, 103–108.

MORA C.F., KWAN A.K.H., CHAN H.C., 1998. *Particle Size Distribution Analysis Of Coarse Aggregate Using Digital Image Processing*. Cement and Concrete Research, 28, 921–932.

MORA C.F., KWAN A.K.H., 2000. *Sphericity, shape factor, and convexity measurement of coarse aggregate for concrete using digital image processing*. Cement and Concrete Research, 30, 351–358.

MONTORO J.J., GONZALEZ E., 1993. *New analytical techniques to evaluate fragmentation based on image analysis by computer methods*. Proceedings of the 4th Int. Symposium Rock Fragmentation by Blasting, Vienna, Austria, 309–316.

ORD A., 1989. *Real time image analysis of size and shape distributions of rock fragments.* Proc. Aust. Int. Min. Metall, 294, 28.

RHOLL S.A., 1993. *Photographic assessment of the fragmentation distribution of rock quarry muckpiles*. Proceedings of the 4th Int. Symposium Rock Fragmentation by Blasting, Vienna, Austria, 501–506.

TASDEMIR A., OZDAG H., ONAL G., 2011. *Image analysis of narrow size fractions obtained by sieve analysis. An evaluation by log-normal distribution and shape factors*. Physicochemical Problems of Mineral Processing, 46, 95–106.

TOBIAS A., THURLEY M.J., CARLSON J.E., 2012. *A machine vision system for estimation of size distributions by weight of limestone particles*. Minerals Engineering, 25, 38–46.

WANG, W.X., 2006. *Image analysis of particles by modified Ferret method – best-fit rectangle*. Powder Technology, 165, 1–10.

XIA W., YANG J., ZHAO Y., ZHU B., WANG Y. 2012a, Improving floatability of taixi anthracite coal of mild oxidation by grinding. Physicochem. Probl. Miner. Process. 48 (2), 393–401.

XIA W., YANG J., ZHU B., 2012b. Flotation of oxidized coal dry-ground with collector. Powder Technology, 228, 324–326.

ZHANG Z.L., YANG J.G., DING L.H., ZHAO Y.M., 2012. An improved estimation of coal particle mass using image analysis. doi:10.1016/j.powtec.2012.06.027.